2016 International Conference on Intelligent Manufacturing and Materials (ICIMM 2016)
ISBN: 978-1-60595-363-2

Preparation of Polyaniline Graphene Carbon Nanotubes Three-dimensional Composites with High Rate Performance

Zhihong Luo, Min Zhu, Yuzhen Zhao, Li Xiang, Chunxia Wang, Kun Luo and Nan Wang

ABSTRACT

Composites of polyaniline (PANI), graphene (RGO) and carbon nanotubes (CNTs) were prepared by *in situ* polymerization. The morphologies of the composites were examined by scanning electron microscopy and transmission electron microscopy, which showed that PANI were coated onto the surface of RGO and CNTs homogeneously and PANI/CNTs were embedded between and/or bridged PANI/RGO sheets. The composites with three-dimensional porous structure possessed higher specific surface area and pore volume compared to those of PANI and PANI/RGO. Such three-dimensional composites exhibited good capacitive performance during the rapid charge-discharge process. The capacitance values of PANI/RGO/CNTs were717 F g^{-1} and 450 F g^{-1} at the current densities of 1mV $s^{-1}$and 200 mV s^{-1}, respectively. The capacitance retention was 62.7% which was higher than that of PANI/RGO and PANI. The cycling performance indicated the long life stability of PANI/RGO/CNTs.

Zhihong Luo, Min Zhu, Yuzhen Zhao, Li Xiang, Kun Luo, Ministry-province Jointly-constructed Cultivation Base for State Key Laboratory of Processing for Non-ferrous Metal and Featured Materials and Guangxi Key Laboratory of Universities for Clean Metallurgy Comprehensive Utilization of Nonferrous Metal Resource, College of Materials Science and Engineering, Guilin University of Technology, Guilin, 541004, PR China
Nan Wang, College of Chemistry and Chemical Engineering, Huazhong University of Science and Technology, Wuhan 430075, PR China

INTRODUCTION

Electrochemical capacitors, also called supercapacitors, are considered to be the intermediate system between traditional dielectric capacitors and batteries due to their fast recharge capability, high power density, long cycle life and low maintenance cost. Conducting polymers and metal oxides are used as pseudo capacitance materials with high capacitance [1-2]. And polyaniline (PANI) is widely used due to its good electrochemical activity, high reversible pseudo capacitance (with a theoretical value of 2000 F g-1), good thermal stability and environmentally friendly property. However, low conductivity and poor electrochemical stability restrict its application. Compounding conductive carbons materials with high stability, the above-mentioned issues of PANI can be improved [3-6]. Among these carbon materials, graphene with fascinating electronic and mechanical properties is a promising materials for various applications, including Nano electronics and energy storage/conversion [7]. The combination of PANI and graphene has been proven to be attractive as a means to reinforce the electrochemical stability of PANI and to increase the capacitance value [8-10].

However, the composite of graphene/PANI prepared by in situ polymerization tends to form a paper-like structure, which may stack together during the post treatment process. Thus, the reduction of ions pathway and active sites leads to the increased resistance of the electrode [11-13]. However, constructing three-dimensional (3D) interpenetrating structure of electrode materials may provide a good solution to the issue of poor electronic and ionic transportation in electrode materials, thereby resulting in high-performance devices. It was reported that graphene or graphene composites with a 3D composite structure can be built by using carbon nanotubes (CNTs) as additives [14-16]. Lu and coworkers adopted polyaniline/carbon nanotube composites as an additive to prepare graphene/polyaniline/carbon nanotube films[17]. However, polyaniline was not deposited onto the graphene surface, the specific capacitance of the composites was not high. Yan and coworkers found that the cycling performance of the graphene/polyaniline composite was improved by using 1% CNTs as a conductive additive[18]. However, the rate performance of GNS/CNTs/PANI needed to be improved. The graphene/CNT-polyaniline composites exhibited high capacitive performance even in an ionic liquid electrolyte[19].

Here, to shorten the ionic and electronic transport paths further, the morphology of PANI was tailored by using ethanol-water solution during preparation process. The combined effect of 3D structure and uniform nanoparticles of PANI could improve the super capacitive performance through shortening the electronic and ionic pathway and increasing the accessible active sites [6, 20-21].The results showed that PANI/RGO/CNT not only exhibited high capacitance and good stability, but also exhibited good performance at high rate charge/ discharge process.

Experimental

Raw materials

Nature flake graphite (99%) was obtained from Qingdao Lihaofeng Graphite Co., Ltd. (Qingdao, China). Raw multi-walled carbon nanotubes 5-15 μm in length and 20-50 nm in diameter were obtained from Shenzhen Nanotech Porch Co., Ltd., China. Aniline was purchased from Sinopharm Chemical Reagent Co., Ltd. (Shanghai, China). All other chemicals were of analytical grade and used as received. Distilled water was used throughout the work.

Preparation of RGO and Functionalized CNTs

96 mg of glucose was added into 120 mL of homogeneous GO dispersion (0.05 mg mL-1). The mixture was stirred for 30 min, and then 100 μL of concentrated ammonia was added into it. After being vigorously stirred for 10 min, the solution was refluxed at 95 °C for 60 min. The obtained RGO was filtered through a nylon membrane filter (0.2 μm) and dispersed into ethanol with a concentration of 0.5 mg mL-1.

CNTs were refluxed in concentrated H2SO4/HNO3 (3/1 v/v) at 70°C for 2 h to produce carboxylic acid-functionalized CNTs and then filtered and washed with distilled water several times. Finally, CNTs powder was obtained by drying the samples at 60 °C for 24 h. The functionalized CNTs were ultrasonically dispersed in ethanol with a concentration of 0.5 mg mL-1.

Preparation of 3D PANI/RGO/CNTs, PANI/RGO and PANI

RGO and CNTs were mixed by sonication at a mass ratio of 4:1, followed by adding aniline (0.3 g), which was dissolved in 5 mL of 1.0 mol L-1HCl solution. The polymerization was performed in an ice bath for 5 h with stirring by adding APS. The composite prepared without using CNTs is denoted as PANI/RGO. And pure PANI was prepared with the same method.

Characterization

All electrochemical measurements were performed in a three-electrode setup. The working electrodes were prepared by drop casting 10 μL of the samples (2 mg mL-1) onto a glassy carbon electrode twice and dried in an oven at 45 °C, Pt wire and saturated calomel electrode (SCE) were used as counter electrode and reference electrode, respectively. The Brunauer-Emmett-Teller (BET) specific surface area was determined by N2 adsorption/desorption using a surface area analyzer (MICROMETERS ASAP 2020). The morphology images of all samples were obtained on field transmission electron microscopy (TEM, Tecnai G2 20s-TWIN) in low vacuum mode.

RESULTS AND DISCUSSION

Morphology and Structure of The Composites

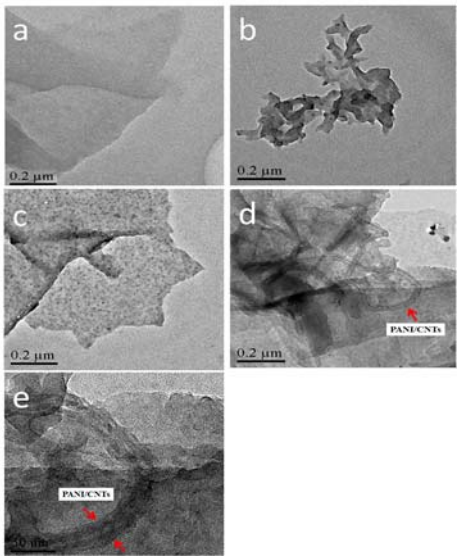

Figure 1. TEM images of RGO (a), PANI (b), PANI/RGO (c) and PANI/RGO/CNTs (d, e).

Morphologies showed in Figure. 1a demonstrated that RGO had a structure of crumpled and curved sheets. Wrinkles were observed on the surface of RGO. As observed from Figure 1b, PANI exhibited a feature of nano-fibrillar structures. For the composites of PANI/RGO (Figure 1c) and PANI/RGO/CNTs (Figure 1d), the paper-like structures were still observed. As shown in Figures 1c and 2d, PANI particles were coated uniformly on the surface of RGO, and the size of the PANI particles was much smaller than that of pure PANI. According to our previous study, the uniformly deposition of PANI was benefit to reduce the internal resistance [6]. For PANI/RGO/CNTs, PANI also grew on the surface of CNTs inferred from its roughness morphology, the diameters of PANI-coated CNTs were approximately 40 nm, and the thickness of PANI layer was approximately 10 nm (Figure 1e).

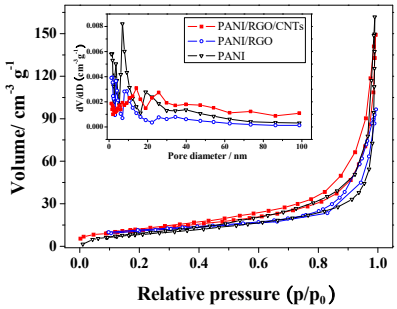

Figure 2. Nitrogen adsorption-desorption isotherm curves of PANI, PANI/RGO and PANI/RGO/CNTs. Inset: Pore size distribution patterns.

The porous structure and Brunauer-Emmett-Teller (BET) specific surface area of pure PANI, PANI/RGO, and PANI/RGO/CNTs were investigated by nitrogen isotherm adsorption (Figure 2). All of the samples exhibit a type IV adsorption-desorption isotherm according to the IUPAC classification, indicating typically mesoporous and/or macro porous structure in the samples due to the capillary condensation the nitrogen molecules in the mesoporous. The surface area of PANI, PANI/RGO and PANI/RGO/CNTs were 31.8, 37.4 and 42.2 m2 g-1, and pore volume was 0.139, 0.065 and 0.160 cm3 g-1,respectively. With the addition of RGO and CNTs, the surface area and pore volume of PANI increased, demonstrating the increasing of active sites. The partly pore volume of PANI/RGO/CNTs arise from the pores mainly distributing in the range from 10 to 60 nm, indicating that PANI/RGO/CNTs has a quite open 3D structure, which was favorable for the access of the electrolyte ions to the inner PANI during the charging/discharging process.

Electrochemical Performances of 3D PANI/RGO/CNTs Composite

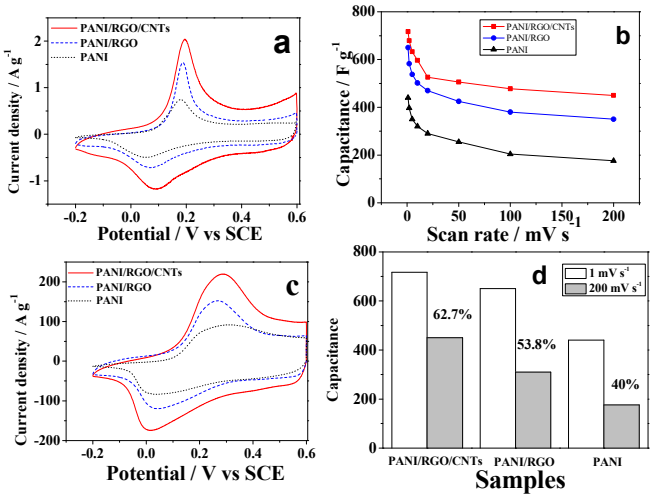

Figure 3. Electrochemical characteristics of PANI, PANI/RGO and PANI/RGO/CNTs. CV curves at 10 mV s^{-1} (a) and at 200 mV s^{-1} (c), specific capacitance at different scan rate (b), capacitance at 1 mV s^{-1} (white bars) and 200 mV s^{-1} (gray bars)(d).

As Figure 3 showed, the CV loops exhibited a pair of redox peaks attributed to leucoemeraldine-emeraldine transition of PANI. PANI/RGO/CNTs exhibited relatively largest current responses, which implied highest specific capacitance. At the scan rate of 1 mV s-1, the capacitance of PANI/RGO/CNTs was 717 F g-1, which was higher than that of PANI/RGO (650 F g-1) and PANI (440 F g-1). The capacitance decreased with the increasing scan rate (Figure 3b). At 200 mV s-1, the capacitance of PANI/RGO/CNTs was still as high as 450 F g-1, which was 128% of PANI/RGO (350 F g-1) and 255% of PANI (176 F g-1). The 3D PANI/RGO/CNTs

composite exhibited higher capacitance at high scan rates, which was more suitable for supercapacitors. Difference of the capacitance at 1 mV s-1(white bar) and 200 mV s-1(gray bar) was showed in Figure 3d. The capacitance retention of PANI/RGO/CNTs(62.7%) was higher than that of PANI/RGO(53.8%) and PANI(40%), which indicated that PANI/RGO/CNTs exhibited better rate performance. The good capacitive performance of the 3D PANI/RGO/CNTs composite at high scan rates became more significant compared to the values of PANI and PANI/RGO. At high scan rates, the shape of the CV curves changed due to the existence of internal resistance. As showed in Figure 3c, The CV curve of PANI was observed to be poorly distorted at 200 mV s-1, which exhibited a rather wide anodic band, while the PANI/RGO/CNTs composite maintained its anodic peak, although it was wider than that at the scan rate of 10 mV s-1. According to the significant deformation of the CV loops at high scan rates, we inferred that the PANI possessed the highest internal resistance.

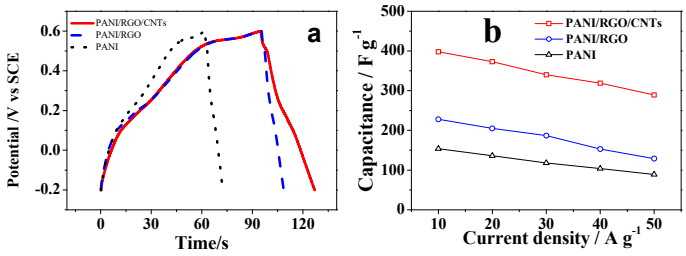

Figure 4. (a) Charge-discharge curves at current densities of 10 A g^{-1}. (b) Specific capacitance at different charge current densities.

As Figure 4(a) showed, the PANI/RGO/CNTs exhibited the longest discharge duration, which indicated the highest specific capacitance. As shown in Figure 4b, at the current density of 10 A g-1, the specific capacitance of PANI/RGO/CNTs, PANI/RGO and PANI were 398, 228 and 154 F g-1, respectively. With the increase in charge-discharge current density, the specific capacitance decreased. However, the capacitance of PANI/RGO/CNTs at each current density was higher than that of PANI/RGO and PANI, possibly because the pore volume of PANI/RGO/CNTs (0.160 cm3 g-1) was larger than that of PANI/RGO (0.065 cm3 g-1) and PANI (0.139 cm3 g-1). At a high current density, the effect of the porous structure on the capacitance became more notable which was in accordance with CV results, demonstrating that such porous structure is essential for rapid penetration of the electrolyte ions into the inner part of electrode materials [11].

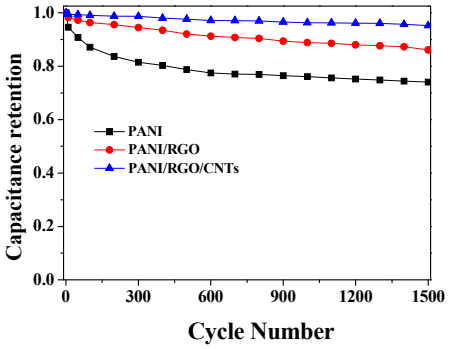

Figure 5. Variation of specific capacitances of PANI, PANI/RGO and PANI/RGO/CNTs as a function of cycle number during the potential scanning range from -0.2 to 0.6 V at 100 mV s^{-1}.

The long life stability of all samples was presented in Figure 5. As the cycling number increasing, the capacitance of PANI decreased rapidly, with a capacitance retention of 74% after 1500 cycles. As for PANI/RGO and PANI/RGO/CNT, the capacitance retention was 86% and 95%, respectively. Compared to PANI/RGO, PANI/RGO/CNT exhibited better cycling performance, possibly due to the porous structure and high conductivity of carbons.

CONCLUSIONS

PANI/RGO/CNTs composites with 3D structures were prepared by in situ polymerization of aniline in the presence of both RGO and CNTs. The morphology characterization indicated that PANI was coated uniformly on the surface of RGO and CNTs, long and tortuous PANI/CNTs intertwined and linked PANI/RGO sheets. PANI/RGO/CNTs with porous structure had higher specific surface area and larger pore volume than PANI/RGO and PANI. The electrochemical measurements proved that the incorporation of CNTs improved the capacitive performance of PANI/RGO, including the specific capacitance, rate performance and long-life cycling stability.

ACKNOWLEDGEMENT

This work was supported by National Natural Science Foundation of China (No. 21163004), the Guangxi Natural Science Foundation (No. 2015GXNSFBA139220 and 2013GXNSFAA019029) and the funding from Guangxi Key Laboratory of Universities for Clean Metallurgy Comprehensive Utilization of Nonferrous Metal Resource and Guangxi Ministry-Province Jointly-Constructed Cultivation Base for State Key Laboratory of Processing for Non-ferrous Metal and Featured Materials.

REFERENCES

1. K. Zhang, L.L. Zhang, X.S. Zhao, Graphene/polyaniline nanofiber composites as supercapacitor electrodes, Chem. Mater., 2010, 22(4): 1392-1401.
2. J.C. Zhao, B.H. Tang, L. Sun, Effect of loading amount on capacitance performances of MnO_2/ordered mesoporous carbon composites. Mater. Tech., 2012, 27(4): 328-332.
3. J. Jang, J.W. Bae, M.J. Choi, Fabrication and characterization of polyaniline coated carbon nanofiber for supercapacitor, Carbon, 2005, 43(13): 2730-2736.
4. W. Fan, C. Zhang, W.W. Tjiu, Graphene-wrapped polyaniline hollow spheres as novel hybrid electrode materials for supercapacitor applications, ACS Appl. Mater. Interfaces, 2013, 5(8): 3382-3391.
5. Y.Z. Li, X. Zhao, P.P. Yu, Oriented arrays of polyaniline Nano rods grown on graphite Nano sheets for electrochemical supercapacitor, Langmuir, 2013, 29(1): 493-500.6.
6. Z.H. Luo, L.H. Zhu, H.Y. Zhang, Polyaniline uniformly coated on graphene oxide sheets as supercapacitor material with improved capacitive properties, Mater. Chem. Phys., 2013,139 (2-3): 572-579.
7. D.A.C. Brownson, D.K. Kampouris, C.E. Banks, An overview of graphene in energy production and storage applications, J. Power Sources, 2011, 196(11): 4873-4885.
8. J. Yan, T. Wei, B. Shao, Preparation of a graphene Nano sheet/polyaniline composite with high specific capacitance, Carbon, 2010, 48(2): 487-493.
9. S.P. Zhou, H.M. Zhang, Q. Zhao, Graphene-wrapped polyaniline Nano fibers as electrode materials for organic supercapacitors, Carbon, 2013, 52: 440-450.
10. J.T. Zhang, X.S. Zhao, Conducting polymers directly coated on reduced graphene oxide sheets as high-performance supercapacitor electrodes, J. Phys. Chem. C, 2012, 116(9): 5420-5426.
11. G.C. Li, Y. Li, H.R. Peng. Synthesis and electrochemical performance of dispersible polyaniline/sulfonated graphene composite Nano sheets, Synth. Met., 2013, 184(15):10-15.
12. P.P. Yu, Y.Z. Li, X. Zhao, In situ growth of ordered polyaniline nanowires on surfactant stabilized exfoliated graphene as high-performance supercapacitor electrode, Synth. Met., 2013, 185-186(1): 89-95.
13. F. Huang, D. Chen, Towards the upper bound of electrochemical performance of ACNT@polyaniline arrays as supercapacitors, Energy Environ. Sci., 2012, 5(2): 5833-5841.
14. S.Y. Yang, K.H. Chang, H.W. Tien, Design and tailoring of a hierarchical graphene-carbon nanotube architecture for supercapacitor, J. Mater. Chem., 2011, 21(7): 2374-2380.
15. Q. Cheng, J. Tang, J. Ma, Graphene and carbon nanotube composite electrodes for supercapacitors with ultra-high energy density, Phys. Chem. Chem. Phys., 2011, 13(39): 17615-17624.
16. L.F. Shen, X.G. Zhang, H.S. Li, Design and tailoring of a three-dimensional TiO_2-graphene-carbon nanotube nanocomposite for fast lithium storage, J Phys. Chem. Lett., 2011, 2(24): 3096-3101.
17. X.J. Lu, H. Dou, S.D. Yang, Fabrication and electrochemical capacitance of hierarchical graphene/polyaniline/carbon nanotube ternary composite film, Electrochim. Acta, 2011, 56 (25): 9224-9232.
18. J. Yan, T. Wei, Z.J. Fan, Preparation of graphene Nano sheet/carbon nanotube/polyaniline composite as electrode material for supercapacitors, J. Power Sources, 2010, 195(9): 3041-3045.
19. Q. Cheng, J. Tang, N. Shinya, Polyaniline modified graphene and carbon nanotube electrode for asymmetric supercapacitors of high energy density, J. Power Sources, 2013, 241(1): 423-428.
20. J.J. Xu, Wang K, Zu SZ, et al. Hierarchical nanocomposites of polyaniline nanowire arrays on graphene oxide sheets with synergistic effect for energy storage [J]. ACS Nano, 2010, 4(9): 5019-5026.
21. B. Ma, X. Zhou, X.W. Li, Hierarchical composites of sulfonated graphene-supported vertically aligned polyaniline Nano rod for high-performance supercapacitors, J. Power Sources, 2012, 215(1): 36-42.